

Supplementary Material of

Adaptive Baseline Finder, a statistical data selection strategy to identify atmospheric CO₂ baseline levels and its application to European elevated mountain stations

Ye Yuan¹, Ludwig Ries², Hannes Petermeier³, Martin Steinbacher⁴, Angel J. Gómez-Peláez⁵, Markus C. Leuenberger⁶, Marcus Schumacher⁷, Thomas Trickl⁸, Cedric Couret², Frank Meinhardt⁹, Annette Menzel^{1,10}

¹Department of Ecology and Ecosystem Management, Technische Universität München, Freising, Germany

²German Environment Agency (UBA), Zugspitze, Germany

³Department of Mathematics, Technische Universität München, Freising, Germany

⁴Empa, Laboratory for Air Pollution/Environmental Technology, Dübendorf, Switzerland

⁵Izaña Atmospheric Research Center, Meteorological State Agency of Spain (AEMET), Santa Cruz de Tenerife, Spain

⁶Climate and Environmental Physics Division, Physics Institute and Oeschger Centre for Climate Change Research, University of Bern, Bern, Switzerland

⁷Meteorological Observatory Hohenpeissenberg, Deutscher Wetterdienst (DWD), Hohenpeissenberg, Germany

⁸Institute of Meteorology and Climate Research, Atmospheric Environmental Research (IMK-IFU), Karlsruhe Institute of Technology (KIT), Garmisch-Partenkirchen, Germany

⁹German Environment Agency (UBA), Schauinsland, Germany

¹⁰Institute for Advanced Study, Technische Universität München, Garching, Germany

Correspondence to: Ye Yuan (yuan@wzw.tum.de)

S1 Applicability of ABF

S1.1 Running frequency of ABF

We compared the ABF derived *start time windows* of overall running frequency with seasonal running frequency, shown in Table S1.1.

Table S1.1: *Start time window* by overall frequency and seasonal frequency (data of whole period), hours in advance and delayed are listed in brackets.

Season	IZO	ZSF	SNB	JFJ
Overall	1 a.m. – 6 a.m.	10 p.m. – 3 a.m.	3 a.m. – 8 a.m.	11 p.m. – 4 a.m.
Winter	2 a.m. – 7 a.m. (+1 hr)	1 a.m. – 6 a.m. (+3 hr)	6 p.m. – 11 p.m. (-9 hr)	3 a.m. – 8 a.m. (+4 hr)
Spring	11 p.m. – 4 a.m. (-2 hr)	10 p.m. – 3 a.m. (0 hr)	5 a.m. – 10 a.m. (+2 hr)	6 p.m. – 11 p.m. (-5 hr)
Summer	1 a.m. – 6 a.m. (0 hr)	0 a.m. – 5 a.m. (+2 hr)	3 a.m. – 8 a.m. (0 hr)	1 a.m. – 6 a.m. (+2 hr)
Autumn	1 a.m. – 6 a.m. (0 hr)	9 p.m. – 2 a.m. (-1 hr)	5 a.m. – 10 a.m. (+2 hr)	0 a.m. – 5 a.m. (+1 hr)

As a result, most of the seasonal derived *start time windows* differ moderately from the overall derived *start time windows*. However, two exceptions have been observed, which are winter at SNB and spring at JFJ. Therefore, graphical examination was taken in Fig. S1.1 (a) and (b).

For winter time at SNB, the seasonal derived *start time window* is with the least standard deviation, but doesn't exhibit the minimal value from the diurnal cycle. For winter, we expect the most representative level of CO₂ to be around the minimal values with relatively small standard deviations. Therefore, the overall derived *start time window* is more suitable to be the ideal *start time window* in this case.

Similar case happens to the spring time at JFJ. For spring, the vegetation activities have been already influenced the CO₂ diurnal cycle. The *start time window* in this case is not suitable as the minimal values included. Again, the overall derived *start time window* is more practical.

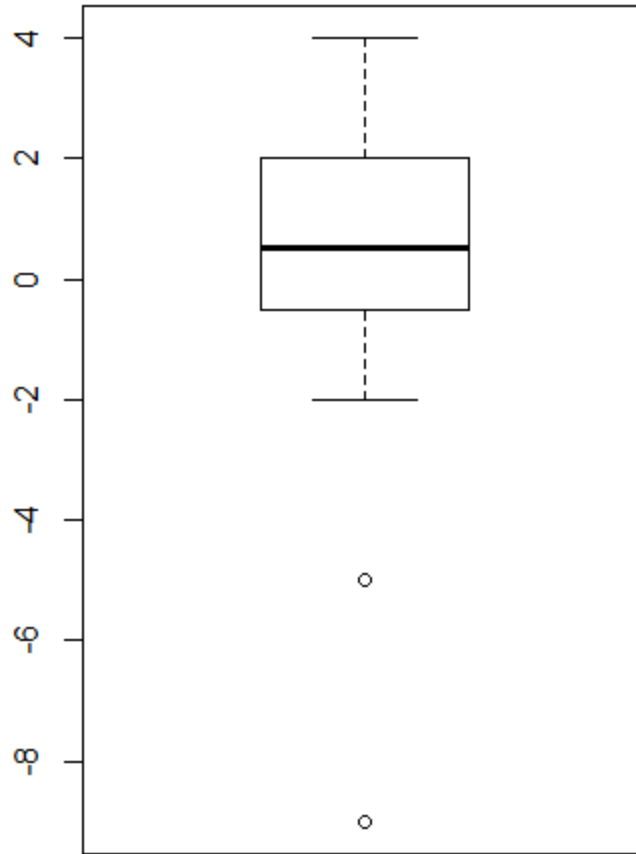


Figure S1.1 (a): Boxplot for hourly shifts of seasonal derived *start time windows* from overall derived *start time windows*, corresponding to Table S1.1.

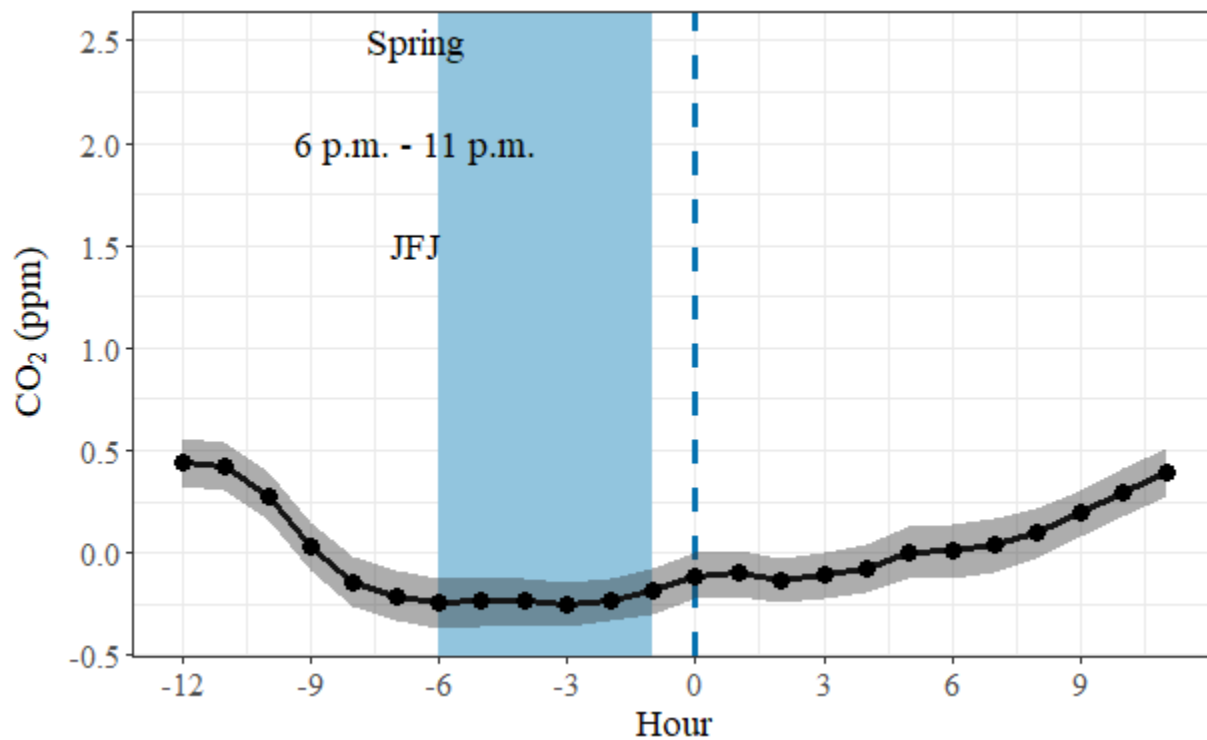
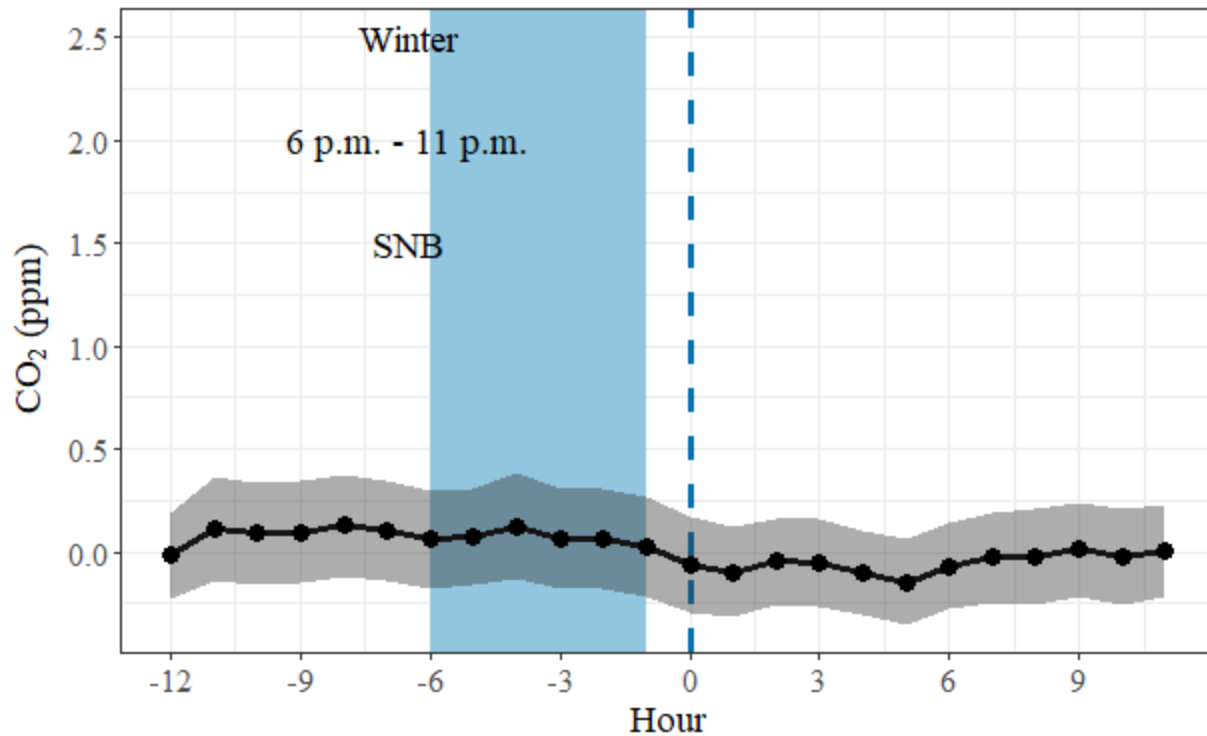


Figure S1.1 (b): Detrended mean diurnal variations of validated CO₂ mole fractions (black) with 95% confidence intervals (grey) for winter time at SNB (upper) and for spring time at JFJ (below). The corresponding seasonal derived *start time windows* are shown both in blue shades and texts.

S1.2 Standard deviation threshold $s_{i,threshold}$

The threshold of standard deviation determines the degree of variation for the selected time windows. In the study, we applied 0.3 ppm to all the stations for inter-comparison. But it is clear that for low elevated stations like SSL, this value may be not appropriate. We tried 1.0 ppm threshold for station SSL and resulted in the same *start time window* and a much higher selection percentage (26.14% compared with 3.8% in the main text), however with a few irregular spikes observed below.

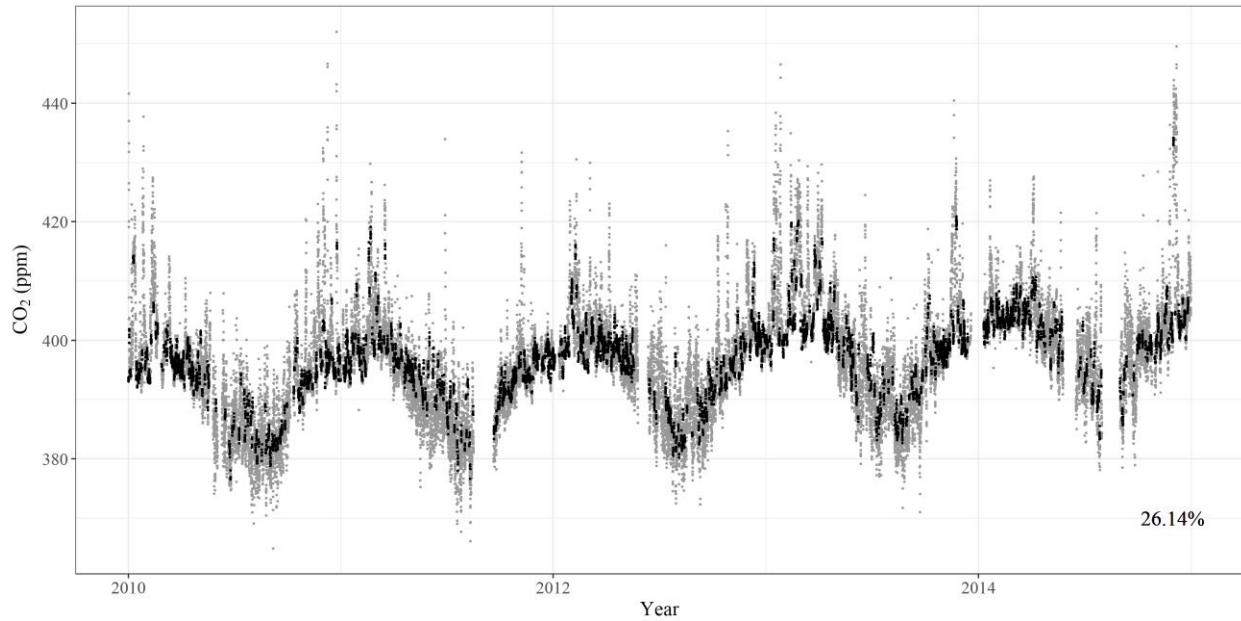


Figure S1.2: Time series plot of validated CO₂ data set (grey) and ABF-selected data set (black) at SSL from 2010 to 2014.

S1.3 Time resolution tr

Data at station ZSF were taken to evaluate the differences in data selection on different time resolution. To compare with the selected result based on hourly averages, we applied ABF directly to the 30-min validated data set. The resulting *start time windows* are the same, but the selection percentages are significantly different at 95% confidence interval, shown in table below.

Table S1.3 (a): Selection percentages by ABF applied to ZSF data sets.

Time resolution	ABF selection percentage \pm 95% confidence interval
30-min	13.46 ± 0.22
1-hour	14.76 ± 0.33

For station JFJ, the 10-min validated data set was available for more detailed comparison. We prepared the ABF-selected data sets on 10-min, 20-min and 30-min time scale to compare with the hourly selected results. The resulting *start time windows* are again the same. The results of selection percentages show again significant differences (at 95% confidence interval) between each two data sets, shown in table below.

Table S1.3 (b): Selection percentages by ABF applied to JFJ data sets.

Time resolution	ABF selection percentage \pm 95% confidence interval
10-min	18.73 ± 0.14
20-min	20.02 ± 0.21
30-min	20.75 ± 0.26
1-hour	22.14 ± 0.37

As a result, these selection percentages clearly indicate a significantly smaller selection percentage with finer time resolution. This can be possibly explained based on the statistical property of ABF. While ABF evaluates the standard deviation within a time window, averaged data with larger time intervals show more statistical robustness. For ABF, it is applicable for data sets with time resolution equal to or finer than one hour.

S2 Detrended diurnal cycles

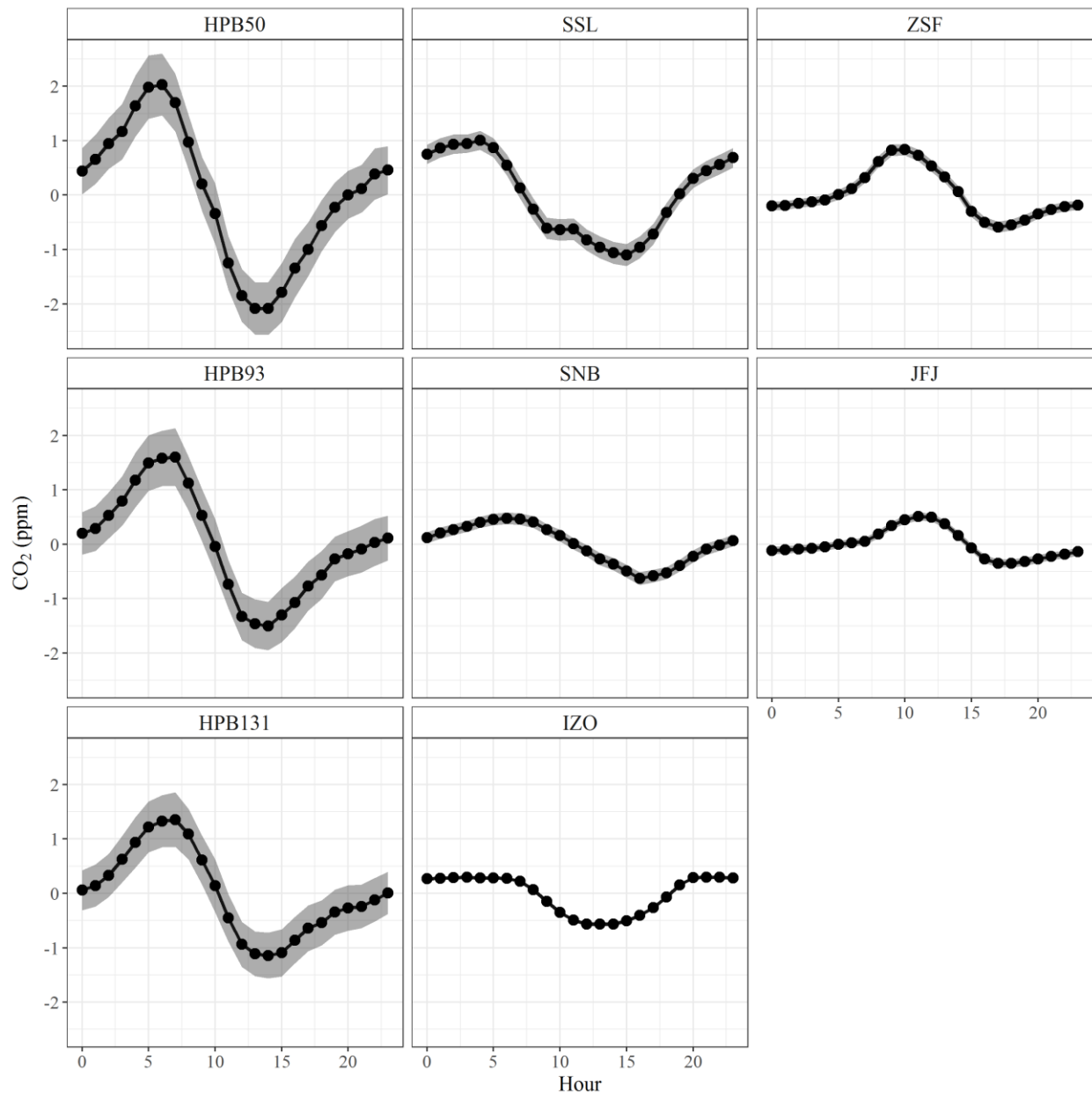


Figure S2: Detrended mean diurnal variation of validated CO₂ mole fractions (black) with 95% confidence intervals (grey) at six European GAW stations.

S3 Selection percentages

S3.1 Table of selection percentages

Table S3.1: List of selection percentages (%) during ABF data selection process (π_1 – selected days with valid *start time window* in all days; π_2 – selected hours with valid *start time window* in all hourly data; π_3 – selected hours after *forward adaptive selection* in all hourly data; ABF – final selection percentages). The bottom shows the linear regression coefficients of stations (*HPB* is represented by *HPB50*; *IZO* is excluded) altitudes and the selection percentages at significance level of 0.05 (*)).**

Station ID	π_1	π_2	π_3	ABF*
<i>HPB50</i>	15.2	2.1	2.6	3.2
<i>HPB93</i>	22.7	3.2	3.9	4.8
<i>HPB131</i>	29.6	4.3	5.2	6.2
<i>SSL</i>	14.0	2.6	3.1	3.8
<i>IZO</i>	85.2	20.0	26.1	36.2
<i>ZSF</i>	52.8	8.9	12.3	14.8
<i>SNB</i>	47.3	10.9	14.9	19.3
<i>JFJ</i>	69.3	12.1	17.4	22.1
Linear regression coefficient (γ^2)	0.941***	0.996***	0.998***	0.996***

*For ABF, the final selection percentage is equivalent to the percentage of selected hours after backward adaptive selection in all hourly data.

S3.2 Linear regression of station altitudes and selection percentages

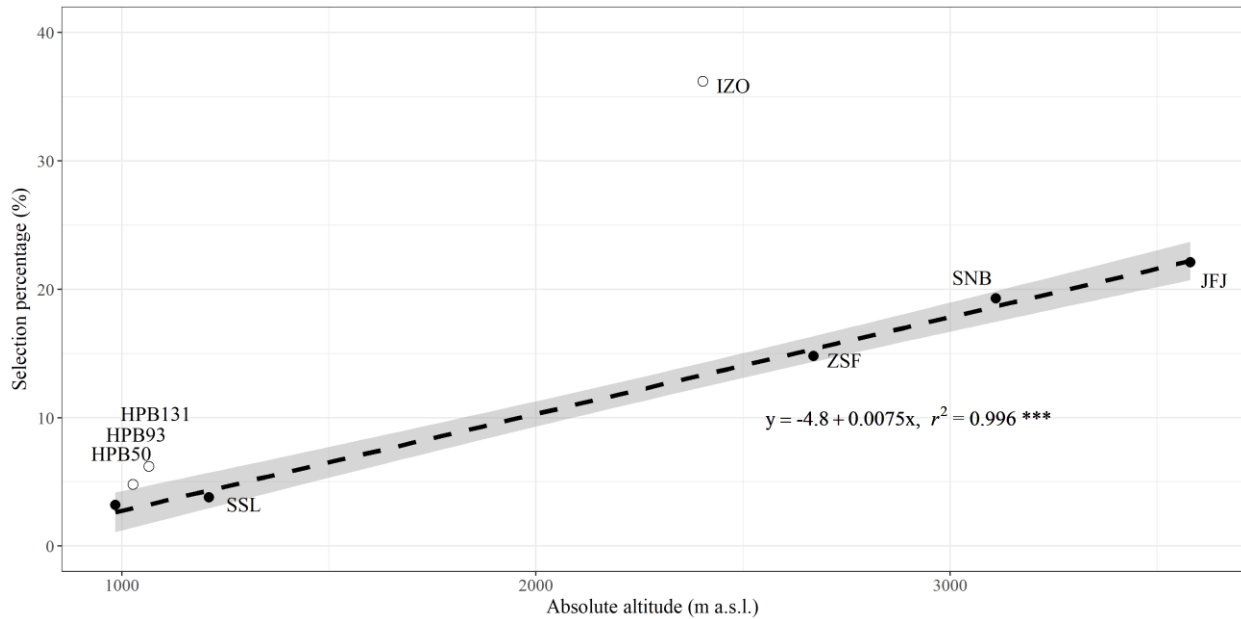


Figure S3.2: Linear regression between the absolute altitudes and the final selection percentages by ABF for all continental sites (excluding *IZO*). For *HPB*, only *HPB50* is chosen as the demonstration sampling height.

S3.3 Comparison of selection percentages among data selection methods

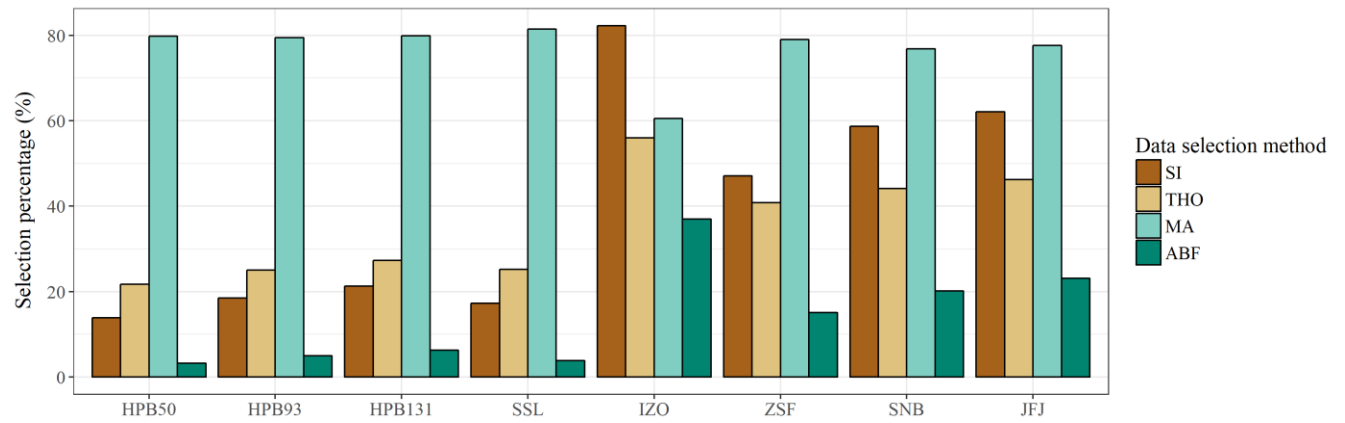


Figure S3.3: Comparison of the selection percentages by four statistical data selection methods (SI, THO, MA, ABF) applied to validated CO₂ data sets at six GAW stations.

S4 Mean monthly variations at SSL, SNB and JFJ

S4.1 SSL

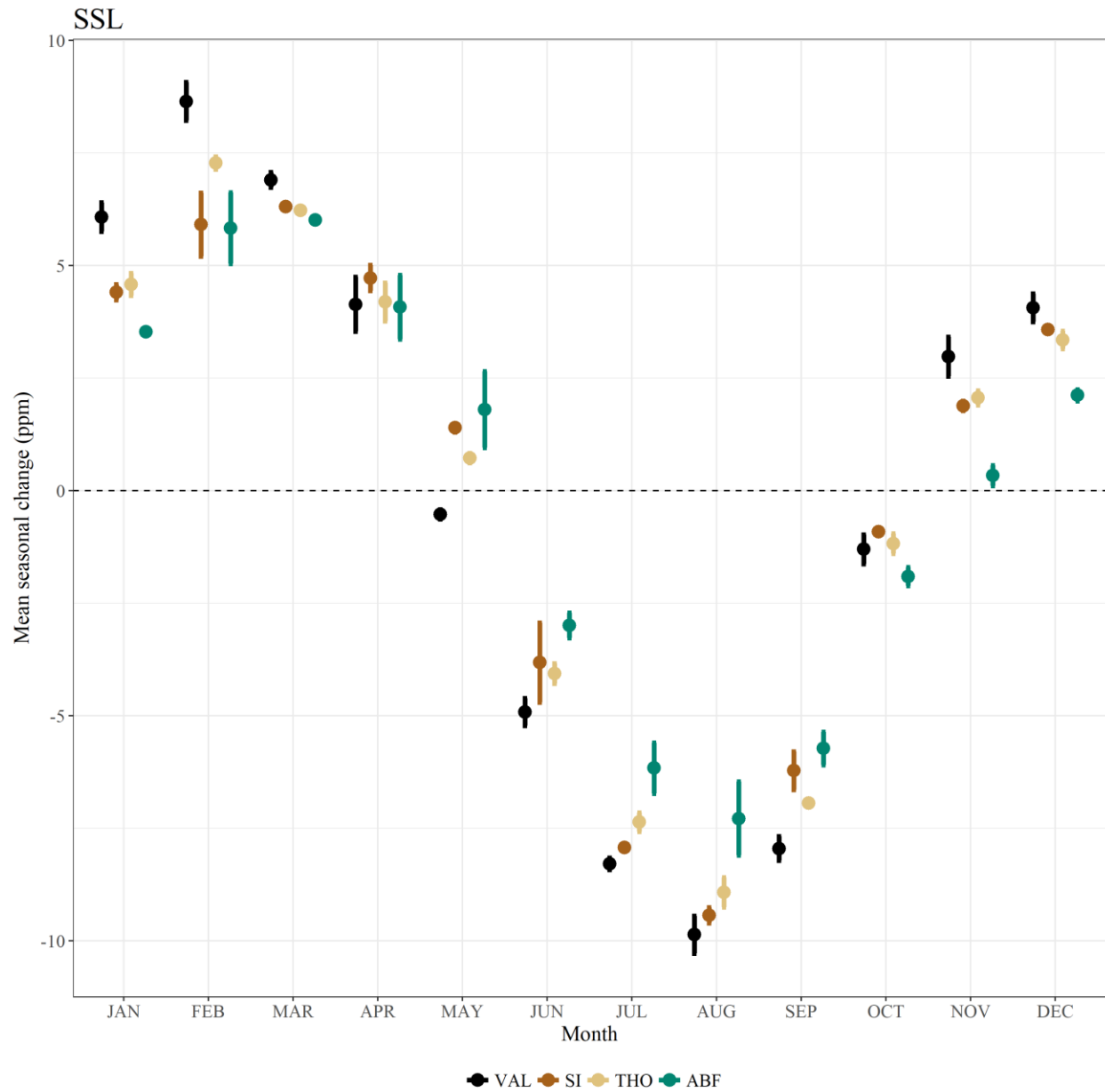


Figure S4.1: Mean monthly variation of the seasonal component decomposed by STL at SSL over the whole time period.

S4.2 SNB

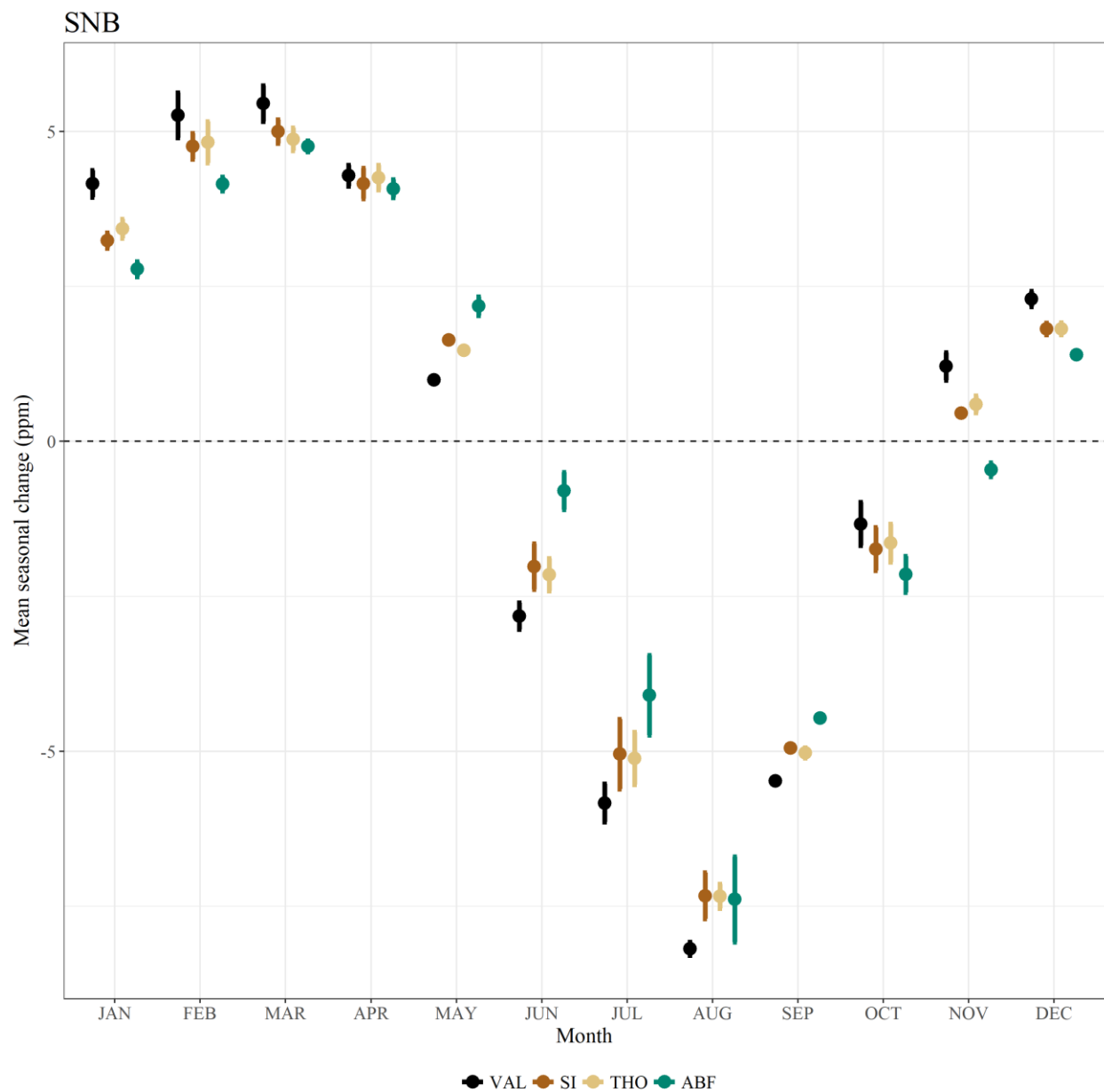


Figure S4.2: Mean monthly variation of the seasonal component decomposed by STL at SNB over the whole time period.

S4.3 JFJ

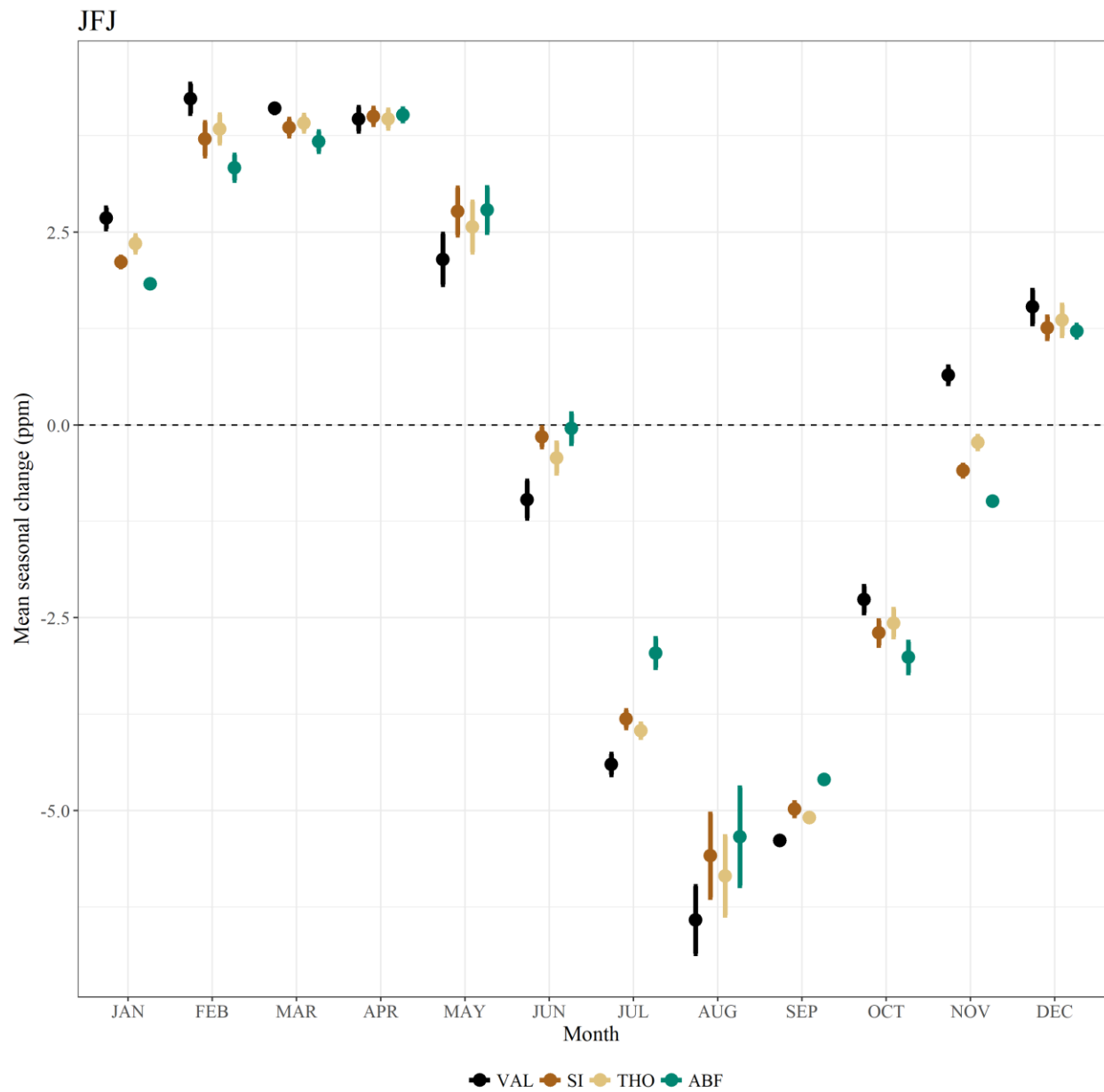


Figure S4.3: Mean monthly variation of the seasonal component decomposed by STL at JFJ over the whole time period.